

BridgeIV: Bridging Customized Image and Video Generation through Test-Time Autoregressive Identity Propagation

Panwen Hu¹, Jiehui Huang², Qiang Sun^{1,3}, Xiaodan Liang^{1,2*}

¹Mohamed bin Zayed University of Artificial Intelligence

²Sun Yat-sen University ³University of Toronto

Abstract

Both zero-shot and tuning-based customized text-to-image (CT2I) generation have made significant progress for storytelling content creation. In contrast, research on customized text-to-video (CT2V) generation remains relatively limited. Existing zero-shot CT2V methods suffer from poor generalization, while another line of work directly combining tuning-based T2I models with temporal motion modules often leads to the loss of structural and texture information. To bridge this gap, we propose an autoregressive structure and texture propagation module (STPM), which extracts key structural and texture features from the reference subject and injects them autoregressively into each video frame to enhance consistency. Additionally, we introduce a test-time reward optimization (TTRO) method to further refine fine-grained details. Quantitative and qualitative experiments validate the effectiveness of STPM and TTRO, demonstrating improvements of 7.8 and 13.1 in CLIP-I and DINO consistency metrics over the baseline, respectively.

1. Introduction

The field of video generation [3, 14, 42, 49] has witnessed remarkable advancements in recent years, with significant breakthroughs in both quality and diversity of generated videos, owing to the enhancement of data quality and the optimization of algorithmic models. Given the inherent uncertainty in generative conditions, several studies have begun to explore conditional generation, such as utilizing image conditions to dictate the initial frame [2, 38, 48], employing layout or contour conditions to govern structural composition [39, 40], and leveraging trajectories or camera poses to regulate motion dynamics [44, 53, 54].

Recently, driven by practical application demands, the generation of long storytelling videos [6, 18, 19] has garnered increasing attention. Distinct from the aforementioned controllable generation approaches, this paradigm necessitates the consideration of content or subject control,

thereby giving rise to personalized video generation. While personalized generation has achieved substantial progress in the realm of image synthesis [9, 31, 47], studies in customized video generation remain relatively limited [32]. Consequently, this paper primarily focuses on the investigation of personalized generation within the video domain.

The objective of Customized Text-to-Video (CT2V) generation is to generate videos that simultaneously satisfy the given textual descriptions and maintain consistency with the reference subject, using text prompts and reference images as inputs. Current CT2V approaches can be broadly categorized into two types: zero-shot methods and fine-tuning methods. Zero-shot methods [13, 20] typically design a generalizable subject feature extractor to capture the identity features, which are then injected into the video generation process. While this approach offers advantages in inference efficiency, zero-shot methods often struggle with generating high-fidelity results for uncommon subjects not seen in the training data. Fine-tuning methods [45] typically follow a Customized Text-to-Image (CT2I) generation strategy, where a model is fine-tuned on several subject images and subsequently inflated to the video domain [4]. However, as shown in Figure 1, directly adapting CT2I models to video generation with the pretrained temporal motion module often results in reduced subject consistency, with the subject’s structure and texture undergoing unintended deformations as the video evolves.



Figure 1. The first row presents the generated customized images, while the second row displays the video result. Although the customized image generation model achieves promising results, directly integrating a temporal motion module leads to structural and texture distortions in the video

*Corresponding author

To bridge the gap between the CT2I model and video generation, we believe that extracting, propagating, and enhancing the subject’s structure and texture are crucial for improving video consistency. Therefore, this paper proposes a framework to solve the challenge from these three aspects. Specifically, our method consists of three stages: the customization stage, the structure and texture injection stage, and the latent enhancement stage. In the customization stage, inspired by mainstream CT2I approaches [25, 26], we adopt texture inversion [9] and DreamBooth [31] techniques to customize a T2I model. In the structure and texture injection stage, we integrate the CT2I model with a pre-trained temporal motion module to generate an initial video. During this process, we propose an autoregressive Structure and Texture Propagation Module (STPM), which consists of a Structure Propagation Module (SPM) and a Texture Propagation Module (TPM). These modules extract the subject’s structure and texture information from the CT2I model and inject them into video frames, ensuring structural and texture consistency throughout the video. In the latent enhancement stage, we propose a Test-Time Reward Optimization (TTRO) method, which iteratively refines the latent distribution of the video by leveraging feature similarity comparison. This approach further enhances the consistency of fine-grained details in the generated subject, improving overall visual coherence in the final video.

We evaluate our proposed model on the publicly available dataset [12] and compare it with existing CT2V methods. Both qualitative and quantitative results demonstrate that our approach achieves state-of-the-art performance in maintaining subject identity consistency, outperforming the baseline with improvements of 7.8 and 13.1 in CLIP-I and DINO consistency metrics, respectively. In summary, our main contributions are as follows:

1. We present a novel three-stage CT2V framework and introduce an innovative Structure and Texture Propagation Module (STPM) that effectively bridges the gap between the CT2I model and video generation.
2. To enhance video quality, we introduce the concept of test-time scaling into CT2V and propose a test-time reward optimization (TTRO) method, which refines the generated results in terms of consistency.
3. Finally, we implement existing CT2V methods and conduct qualitative, quantitative, and ablation experiments on the public benchmark to demonstrate the effectiveness and superiority of the proposed method.

2. Related work

Customized text-to-video (CT2V) generation aims to produce video content that closely aligns with a given reference image and textual description by integrating both inputs. With the remarkable advancements in customized text-to-image (CT2I) generation [7, 11, 12, 22], CT2V

has garnered increasing attention. Existing CT2V methods can be categorized into three main approaches: zero-shot approaches, tuning-based methods—both of which have been introduced in CT2I—and a two-stage approach. The two-stage approach [19, 55] typically consists of a CT2I model followed by an image-to-video (I2V) generation model [2, 29, 48]. For example, VideoStudio [23] first trains a zero-shot CT2I model to generate customized images and subsequently employs a dedicated I2V model to animate the generated images into videos. Similarly, any existing CT2I model [7, 11, 12, 22] can be combined with an I2V model to form a two-stage pipeline. However, the limited generalization capability of I2V models often leads to unexpected subject deformations during the animation process.

To enhance the consistency of customized subjects in videos, zero-shot approaches [13, 20] adopt a single-stage framework that directly generates videos from a reference image and a text prompt. Methods in this category, such as VideoBooth [20], typically collect large-scale datasets to train a general identity feature extractor. The extracted features are then injected into the backbone network through specialized mechanisms, and the feature extractor and the backbone network will be trained in an end-to-end manner. While these approaches offer significant advantages in generation efficiency, they come with high training costs and limited generalization ability. As a result, their performance deteriorates when dealing with uncommon subjects.

Another category is the tuning-based approach [4, 5, 21, 43, 46], which we adopt in our method and currently demonstrates superior fidelity in CT2V. Some methods, such as DreamVideo [45], directly train a token embedding and an adapter on a video model using customized images. However, training a video model with image data often leads to overfitting, causing the loss of motion information. Another class of methods, such as Magic-Me [24], first trains a CT2I model and then integrates it with a pre-trained motion module, enabling direct video generation. However, the gap between CT2I model and video generation leads to subject deformation and texture loss in the generated videos. To bridge this gap, we propose an autoregressive Structure and Texture Propagation Module (STPM) that injects and propagates the structure and texture information of the reference subject across all video frames in an autoregressive manner. Furthermore, to enhance fine-grained detail consistency, we introduce a test-time reward optimization method to refine the latent distribution of the generated videos.

3. Preliminary

3.1. Latent Diffusion Model

Our method is built upon a spatiotemporal decoupled text-to-video (T2V) model, AnimateDiff [10], which is inflated from the text-to-image (T2I) model, Stable Diffusion [30], by incorporating temporal motion module behind the original spatial blocks. Consequently, our approach follows the conventional training and generation pipeline of latent diffusion models (LDMs) [30].

Specifically, during the first stage, i.e., the customization stage, we finetune a text embedding and the model parameters on the T2I model using the text inversion [9] and Dreambooth [31] methods. A subject image I is first encoded into a latent representation z_0 using an image encoder. This latent representation z_0 is then corrupted with Gaussian noise ϵ and noise level t through a forward diffusion process, forming a noisy latent representation z_t . The diffusion model subsequently takes the noisy latent representation z_t and a text condition c containing a special subject token $\langle S^* \rangle$ as input, aiming to predict the noise ϵ added to the original latent representation.

Thus, the training objective of the diffusion model is formulated as:

$$\mathbb{E}_{z_0, c, \epsilon, t} [\|\epsilon_\theta(z_t, c, t) - \epsilon\|] \quad (1)$$

where ϵ_θ represents the model prediction. During inference, a random Gaussian noise \hat{z}_T is sampled and fed into the diffusion model, which predicts the noise component. This predicted noise is then utilized to iteratively denoise \hat{z}_T through the reverse diffusion process, progressively refining the latent representation for $t = T, \dots, 1$ to get the hidden representation \hat{z}_0 of the sampled image. This process is formulated as:

$$\hat{z}_{t-1} = \frac{1}{\sqrt{\alpha_t}} (\hat{z}_t - \frac{1 - \alpha_t}{\sqrt{1 - \bar{\alpha}_t}} \epsilon_\theta(\hat{z}_t, c, t)) + \sigma_t \epsilon, \quad (2)$$

where $\sigma_t = \frac{1 - \bar{\alpha}_{t-1}}{1 - \bar{\alpha}_t} \beta_t, \beta_t = 1 - \alpha_t$.

3.2. Cross-attention and Self-attention

Our base model, AnimateDiff [10], employs a UNet architecture that includes cross-attention modules, self-attention modules, and motion modules. Motion modules process features along the temporal dimensions, while the injection of conditional information, such as text prompts, and the feature aggregation primarily rely on cross-attention and self-attention modules [33], respectively. In the cross-attention module, the hidden latents are projected as queries Q , while the condition embeddings are projected as keys K and values V . The latents are then updated through the cross-attention mechanism:

$$CA(Q, K, V) = \text{Softmax}\left(\frac{QK^T}{\sqrt{d}}\right)V$$

Here, d refers to the channel dimensions, $\text{Softmax}()$ is applied over the keys for each query so that the condition information encoded in the projected value matrix V is selectively injected into hidden latents. Meanwhile, by inspecting the attention map $A = KQ^T/\sqrt{d}$, we can identify the regions in the hidden latents that correspond to each condition token, such as the special reference subject token $\langle S^* \rangle$. Thus, analyzing the distribution of the attention map associated with $\langle S^* \rangle$ allows us to assess the structure information of the reference subject [1, 15]. This insight can be leveraged to optimize the hidden latents to enhance subject fidelity.

On the other hand, the self-attention module employs an attention strategy similar to that of the cross-attention module to aggregate features. In the self-attention module, the queries, keys, and values are all derived from hidden features, enabling a high degree of editability. As analyzed in previous works [35, 37], the self-attention module controls the appearance attributes, such as color and texture, through the values V .

4. Method

Given a set of N reference images $\mathbf{I} = \{I_n\}_1^N$ and a target text prompt c containing a special token $\langle S^* \rangle$, the objective of customized text-to-video (CT2V) generation is to generate a video $V = \{F_f\}_{f=1:J}$ that faithfully incorporates the reference subject $\langle S^* \rangle$ while adhering to the given text prompt c . J is the number of video frames F_f . Training-based (zero-shot) methods typically generate videos by conditioning on one or more reference images. However, these approaches rely on large-scale annotated datasets for training and exhibit poor generalization to unseen objects. Another line of zero-shot approaches [13, 20] leverage advanced customized text-to-image (CT2I) generation methods [7, 12] first to synthesize subject-specific images, which are then animated using an off-the-shelf image-to-video (I2V) model [2, 48]. However, the effectiveness of this two-stage pipeline is heavily dependent on the I2V model’s capability, and current I2V models struggle with animating rare or complex objects.

To improve generalization, recent methods explore tuning-based solutions, where a customized video generation model is fine-tuned using only a few reference images \mathbf{I} . Our method follows this paradigm but differs in several key aspects. Existing approaches [45] either fine-tune the entire video model using images—leading to the loss of motion dynamics—or only fine-tune the embedding of a special token $\langle S^* \rangle$ [24], which limits the model’s ability to accurately represent the subject. To address this issue, we propose a three-stage framework for CT2V, including the customization stage, the structure and texture injection stage, and the latent enhancement stage. At the customization stage, inspired by CT2I generation, we employ text in-

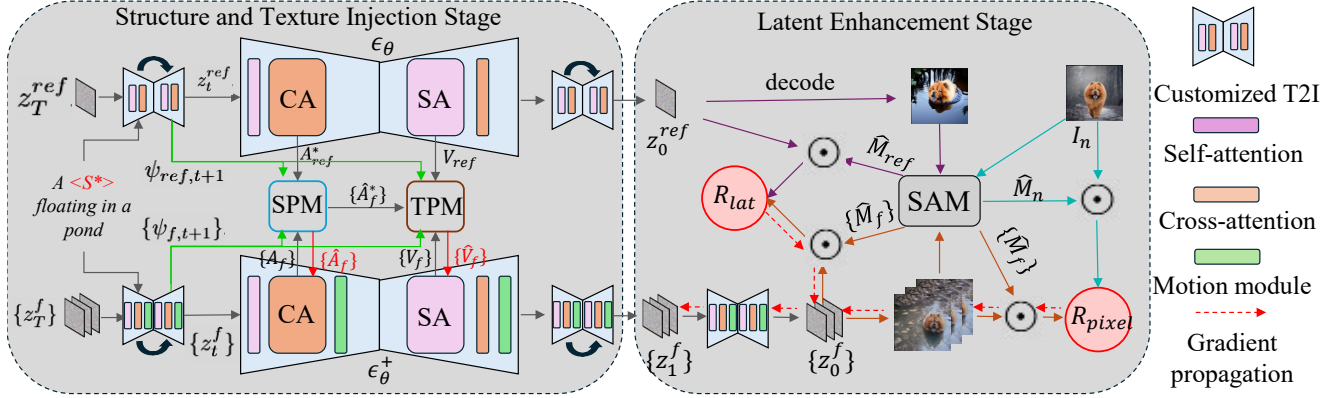


Figure 2. The processes of the structure and texture injection stage (the second stage) and the latent enhancement stage (the third stage). In the second stage, SPM extracts the reference subject’s structure information A_{ref}^* from the cross-attention of the CT2I model and propagates it to video frames through $\{\hat{A}_f\}$, using matching flows computed from the features, $\psi_{ref,t+1}$ and $\{\psi_{f,t+1}\}$ of the previous denoising step. Similarly, TPM utilizes the structure information $\{\hat{A}_f\}$ and matching flow to transfer the reference subject’s texture information V_{ref} into the video. In the third stage, two reward functions are designed in the latent and pixel domains, respectively, to correct the latent distribution, enhancing the consistency of the foreground.

version [9] and Dreambooth [31] techniques to train a customized T2I model ϵ_θ . This process learns the embeddings of the special token $\langle S^* \rangle$ and the customized weights of the T2I model ϵ_θ .

Although the T2I model ϵ_θ at this stage can generate high-quality customized images, the modality gap between image and video domains remains a challenge. Directly adding pre-trained temporal motion modules to ϵ_θ to form the video model ϵ_θ^+ alters the subject’s structural and texture distributions, leading to a decline in subject consistency across generated video frames [4]. To bridge this modality gap, as shown in Figure 2, we propose a novel autoregressive Structure and Texture Propagation Module (STPM), which includes a Structure Propagation Module (SPM) and a Texture Propagation Module (TPM), in the structure and texture injection stage. This module maximally transfers the structural and texture information from the generated reference images to every frame during video generation, while maintaining the smoothness of the video.

Due to the potential loss of fine-grained subject details (e.g., local colors) between the generated image and the original reference images \mathbf{I} , the texture information extracted from the generated image may sometimes be insufficient to ensure that the subject in the video aligns perfectly with the subject in \mathbf{I} . To address this issue, we propose a Test-Time Reward Optimization (TTRP) method in the third stage, which further refines the video latent representation, ensuring that the generated subject continuously approaches the true subject.

4.1. Structure and Texture Propagation

Structure Propagation To enhance the consistency between the video subject structure and the reference subject structure, we need to explore two key aspects: how

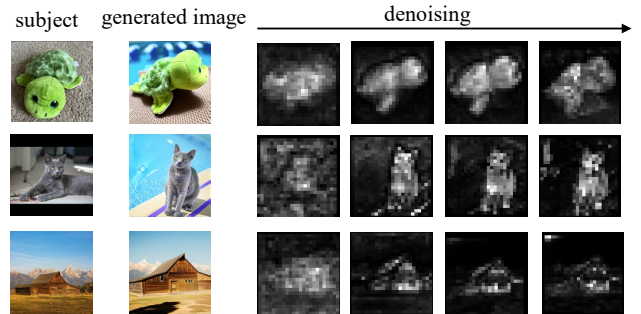


Figure 3. The visualization of normalized attention maps of the special token in different denoising steps. The highlighted regions in the attention maps correspond to the generated reference image (second column), indicating that the attention maps clearly capture the subject’s structural information.

to extract structural information and how to inject structural information. From the cross-attention map shown in Figure 3, we observe that in the T2I model ϵ_θ , the cross-attention modules play a significant role in shaping the subject’s structure. Therefore, we extract the attention map corresponding to the special token $\langle S^* \rangle$ as the structural information and autoregressively inject it into each video frame through a semantic matching flow $o^{F_i \rightarrow F_j}$, which is a displacement field [8, 16, 36] used to warp the subject in F_i to match the subject in F_j .

When extracting structural information, we enhance structural diversity by extracting it from the generated image F_{ref} . Specifically, let i^* denote the position of $\langle S^* \rangle$ in the target prompt c , for each denoising timestep t , the corresponding subject structure distribution $A_{ref,l}^* \in \mathbb{R}^{h_l * w_l \times 1}$ can be obtained from the cross-attention map $A_{ref,l} = Q_{ref,l} K_{ref,l}^T / \sqrt{d}$, $A_{ref,l} \in \mathbb{R}^{h_l * w_l \times L}$ of ϵ_θ as $A_{ref,l}^* =$

$A_{ref,l}[:, i^*]$, where l, L represent the layer number of the attention map and the length of target prompt tokens, respectively, and h_l, w_l represent the height and the width of $Q_{ref,l}$, respectively. For simplicity, we will omit the layer notation l in the following mathematical formulas. Then the target structure $\{A_f^*\}_{f=1:J}$ by autoregressive warping using the matching flow $\{o^{F_i \rightarrow F_j}\}$,

$$A_f^* = \begin{cases} Warp(A_{ref}^*, o^{F_{ref} \rightarrow F_f}), & \text{if } f = 1, \\ Warp(A_f^*, o^{F_f \rightarrow F_{f+1}}), & \text{otherwise.} \end{cases} \quad (3)$$

Consequently, the final cross-attention maps $\{A_f\}_{f=1:J}, A_f \in \mathbb{R}^{h*w \times L}$ for the video V in ϵ_θ^+ are obtained by concatenation operation $concat()$,

$$\hat{A}_f = concat(A_f[:, 1 : i^*], A_f^*, A_f[:, i^* :]). \quad (4)$$

Thus, the output of the cross attention blocks in ϵ_θ^+ becomes $\{Softmax(\hat{A}_f)V_f\}_{f=1:J}$. Through the above process, the structural information can be seamlessly and smoothly injected into the video frames.

Matching Flow Matching flow is the key to successfully injecting structural information. In our framework, we adopt a standard semantic matching workflow [16, 36] to compute the matching flow between two image frames. These conventional pipelines rely on a pretrained feature extractor to extract features from image pairs and subsequently compute their correspondence. However, finding good features under the diffusion framework is not trivial due to the noisy nature of video frames and reference images in the reverse diffusion process.

To address this issue, inspired by previous works [34, 51], we focus on the features from the second-to-last decoder layer of the denoising U-Net ϵ_θ (and ϵ_θ^+), considering its spatial size and the richness of semantic information. Feature maps with excessively high resolution (from higher decoder layers) lead to excessive computational costs, while those with overly low resolution contain insufficient semantic information. let $\psi_{f,t+1} \in \mathbb{R}^{h \times w \times d}$ denote the features of frame F_f at denosing timestep $t + 1$, then the matching cost $C_{t+1} \in \mathbb{R}^{(h \times w) \times (h \times w)}$ between the frame pair is computed as the cosine similarity between the feature vectors of all positions, which is formulated as:

$$C_{t+1}^{f \rightarrow f+1}[i, j] = \frac{\psi_{f,t+1}(i) \cdot \psi_{f+1,t+1}(j)}{\|\psi_{f,t+1}(i)\| \|\psi_{f+1,t+1}(j)\|}, \quad (5)$$

where $i, j \in [0, h) \times [0, w)$, and $\|\cdot\|$ denotes $l - 2$ normalization. Subsequently, we derive the matching flow $o_t^{F_f \rightarrow F_{f+1}} \in \mathbb{R}^{h \times w \times 2}$ used at time step t by applying argmax operation [8] on $C_{t+1}^{f \rightarrow f+1}$. It is worth noting that when computing the matching flow for attention maps of different resolutions, we interpolate the features to the corresponding resolution before calculating the matching cost.



Figure 4. The visualization of the warping results with the matching flows. The first column represents the generated reference image, its foreground mask, and the results after multiplying with the attention map. (a) The corresponding generated video frames. (b) The warping results from the previous frame. (c) The warped foreground masks. (d) The warping results multiplied with the attention maps. We can observe that the subject from the reference image or video frame is correctly warped to the appropriate position in the next frame, providing the subject’s texture information.

Texture Propagation In addition to structural information, the texture details of the subject may also be lost during the transition from the image modality to the video modality. To address this, we propose an autoregressive texture propagation module (TPM) to propagate the reference subject’s texture information across video frames. Previous research [1] has shown that self-attention module plays a crucial role in integrating texture information stored in the value variable. Therefore, our TPM enhances the values $\{V_f\}_{f=1:J}, V_f \in \mathbb{R}^{(h \times w) \times d}$ of the self-attention module. Specifically, we first inject the reference texture into the first frame of the video using the matching flow $\{o\}$ introduced above. Then, the texture is gradually propagated to the subsequent frames of the video. Thus, the enhanced values \hat{V}_f for each frame is computed as:

$$\hat{V}_f = \begin{cases} Warp(V_{ref}, o^{F_{ref} \rightarrow F_f}), & \text{if } f = 1, \\ Warp(V_f, o^{F_{f-1} \rightarrow F_f}), & \text{otherwise.} \end{cases} \quad (6)$$

However, a straightforward warping operation may introduce inconsistencies in the appearance of elements outside the subject, such as background variations. Therefore, it is crucial to effectively isolate the subject from the background to ensure that texture propagation affects only the subject region.

To achieve this, we leverage the cross-attention map \hat{A}_f^* of the special token as a soft foreground mask to filter out background information. Specifically, let M_f denote the soft foreground mask computed at frame f , which can be derived by applying a minmax norm on the cross-attention map \hat{A}_f^* , then we employ this mask to selectively blend the propagated texture features, ensuring that only the sub-

ject region is influenced while preserving background in the original frame. The value \hat{V}_f is updated as :

$$\hat{V}_f = \text{Warp}(V_{f-1}, o^{F_{f-1} \rightarrow F_f}) \odot M_f + V_f \odot (1 - M_f)$$

$$M_f = \text{norm}(\hat{A}_f^*),$$

where \odot represents the Hadamard product [17]. Subsequently, the updated values will replace the original values to complete the self-attention computation $\text{Softmax}(Q_f K_f^T / \sqrt{d}) \hat{V}_f$. It is worth noting that, as is typically the case in U-Net, the self-attention module appears before the cross-attention module in each block. Therefore, the cross-attention map used by the self-attention module comes from the previous cross-attention module, whereas the first self-attention module retains the original computation unchanged.

4.2. Test-time Reward Optimization

The STPM is performed at each denoising step. However, in the early time steps, the attention map and the values in the self-attention and cross-attention modules are noisy and lack fine-grained subject details. As a result, in the generated video, there still exists a certain discrepancy in the fine-grained details of the object compared to the original reference image. Therefore, in the third stage of our method, to correct this discrepancy, we propose a Test-Time Reward Optimization (TTRO) approach to refine the distribution of the latent representation to maximize the designed reward functions.

Let $\{z_{f,0}\}$ denote the latent representation obtained from the DDIM denoising [33] in the second stage. Before the correction, we perform a diffusion forward process to obtain the noisy latent $\{z_{f,1}\}$, which is then fed into the model ϵ_θ^+ to predict the noise ϵ , and the new latents $\{\hat{z}_{f,0}\}$ are computed with Eq.2. Similarly, the new latents $\hat{z}_{ref,0}$ of the generated reference image can be obtained in the same manner. Intuitively, the subject region in the new latent $\hat{z}_{f,0}$ is expected to closely match the subject region of the reference latent $\hat{z}_{ref,0}$. Therefore, we propose using the cosine similarity of the average latents in their respective regions as the reward function, where the subject region \hat{M}_f is identified by applying the segmentation method grounding-SAM [28] on the images decoded from the latents. The latent reward function can be written as:

$$R_{lat} = \sum_{f=1}^J \frac{\text{mean}(\hat{z}_{f,0} \odot \hat{M}_f) \cdot \text{mean}(\hat{z}_{ref,0} \odot \hat{M}_{ref})}{\|\text{mean}(\hat{z}_{f,0} \odot \hat{M}_f)\| \|\text{mean}(\hat{z}_{ref,0} \odot \hat{M}_{ref})\|},$$

where $\text{mean}()$ denotes the average function along the spatial dimension, and only the foreground region, i.e., $\hat{M} = 1$, is counted.

In addition to the latent domain, we further measure the reward in the pixel domain by using the off-the-shelf CLIP

model [27] $\text{Clip}()$ to optimize the latents. We can obtain the frames $\{F_f\}$ in pixel domain by decoding the latents $\{\hat{z}_{f,0}\}$ with the pretrained VAE decoder [14]. Then, we measure the clip score between the generated frames and the original customized images I_n , and the reward function in pixel domain is formulated as:

$$R_{pixel} = \frac{1}{JN} \sum_f \sum_n \text{Clip}(F_f \odot \hat{M}_f, I_n \odot \hat{M}_n).$$

Finally, the noisy latent $\hat{z}_{f,1}$ is updated as follow:

$$\hat{z}_{f,1} = \hat{z}_{f,1} + \lambda \nabla_{\hat{z}_{f,t}} (R_{lat} + R_{pixel})$$

By iterating this process continuously, the reward value gradually increases, indicating that the subject in the video inferred from $\{\hat{z}_{f,1}\}$ becomes increasingly similar to the reference subject.

5. Experiment

5.1. Experimental Settings

Dataset. To validate the effectiveness of the proposed method, we conducted experiments using a dataset, Vico [12], for evaluating the customized T2I task. Vico dataset was collected from previous datasets and consists of 16 customized subjects, each containing 4 to 8 images. Additionally, we employed a more challenging set of prompts provided by [25], which includes 24 prompts featuring large displacement, occlusion, and novel-view synthesis. In our experiments, we generated 4 videos for each prompt, resulting in a total of 1,536 videos for evaluation.

Comparison Methods. In this experiment, we categorize the baseline methods into three groups: two-stage methods, zero-shot methods, and tuning-based methods. The two-stage methods include VideoStudio [23] and two additional approaches that first generate images using a customized T2I model and subsequently synthesize videos using an I2V model, specifically CogVideoX. For this category, we employ text inversion + DreamBooth (TI-DB) and MS-Diffusion [41] as the T2I models. The zero-shot methods include VideoBooth [20] and SSR-Encoder [52], where SSR-Encoder was originally designed for the customized T2I task but can be adapted for video generation by integrating Animatediff’s motion module. Additionally, we compare our approach with Magic-Me [24] and DreamVideo [45], which adopt a similar tuning-based strategy. By evaluating our method against these diverse approaches, we aim to comprehensively demonstrate its effectiveness in customized video generation.

Evaluation Metrics. To evaluate the subject customization capability of our method, we adopt three evaluation metrics following prior work [43, 45]. CLIP-T [27] measures text-image alignment by computing the average cosine similarity between the CLIP image embeddings of all generated frames and the corresponding text embedding. CLIP-I



Figure 5. The comparisons with different state-of-the-art CT2V methods, including two-stages methods, VideoStudio [23] and the baseline TI-DB, tuning-based method, Dreamvideo [45], and zero-shot method, Videobooth [20]. It can be observed that the two-stage method is prone to structural deformation, while traditional tuning-based and zero-shot methods have weak representation capabilities for unique objects, resulting in poor consistency in the generated results.

assesses visual similarity by calculating the average cosine similarity between the CLIP image embeddings of all generated frames and the embeddings of the original subject images. Additionally, DINO-I [31] serves as an alternative metric for visual similarity, where we utilize ViT-S/16 DINO [50] to extract embeddings from all generated frames and reference images and compute their cosine similarity. These metrics collectively provide a comprehensive evaluation of both semantic alignment and visual fidelity in the generated customized videos.

Method	Type	CLIP-T \uparrow	CLIP-I \uparrow	DINO \uparrow
TI-DB	T.	29.8	72.2	49.5
MS-Diffusion	T.	28.8	70.4	42.1
VideoStudio	T.	30.1	75.0	56.9
SSR-Encoder	Z.	28.6	77.8	59.9
VideoBooth	Z.	27.8	71.4	49.9
Magic-Me	F.	28.4	77.6	59.0
DreamVideo	F.	30.2	72.4	47.2
Ours	F.	31.7	80.0	62.6

Table 1. The quantitative results of different methods. T., Z., and F. indicate two-stage method, zero-shot method, and tuning-based method, respectively. It can be observed that our method achieves the highest performance on all metrics.

5.2. Comparisons

Table 1 and Figure 5 summarize the quantitative and qualitative comparisons with different state-of-the-art methods. The two-stage approach relies on two separate models: a CT2I model and an I2V model. However, due to the modality gap, they often fail to integrate seamlessly, particularly when dealing with uncommon subjects. As shown in the results of VideoStudio [23] and TI-DB in Figure 5, the I2V model struggles to fully comprehend the structural integrity of the subject, e.g., the shape of the dog’s face and ears, leading to deformation or physically implausible motion. In contrast, our approach maintains better temporal smoothness, and its consistency with the reference subject is effectively demonstrated by the CLIP-I and DINO scores. Our method outperforms the two-stage approach by 5 and 5.7 in CLIP-I and DINO scores, respectively.

Zero-shot approach, e.g., VideoBooth [20], demonstrates strong temporal smoothness. However, it struggles to accurately represent the customized subject, leading to significant texture and structural discrepancies between the generated video and the reference subject. These methods rely on feature extractors trained on large-scale datasets, but inherent data biases limit their generalization to uncommon categories. In contrast, our proposed method incorporates a



Figure 6. The visualization of the generated videos with different combination of components. It can be observed that SPM helps alleviate the structure deformation problem, TPM can enhance the texture consistency, and the reward optimization forces the color of the generated subject to approach that of the reference subject.

dedicated structure and texture propagation module, ensuring superior structural and texture consistency compared to zero-shot approaches. As a result, our method outperforms the best zero-shot approach by 2.2 and 2.7 points in CLIP-I and DINO scores, respectively.

Finally, we compare our approach with tuning-based methods, namely Magic-Me [24] and DreamVideo [45]. Magic-Me represents the customized subject using only a single token embedding, resulting in insufficient representational capacity and poor alignment with the reference subject. On the other hand, DreamVideo directly trains an adapter on a video model using image data, which compromises motion quality. In contrast, our method not only fine-tunes the entire model to enhance representational capacity but also autoregressively propagates structural and texture information across frames. This ensures both subject alignment and motion consistency, achieving a balanced and superior performance.

5.3. Ablation Study

We conducted ablation studies to further validate the effectiveness of the proposed structure and texture propagation module, as well as the test-time optimization. The results are presented in Table 2 and Figure 6. Our baseline method is built upon Text Inversion and DreamBooth, incorporating the motion module from AnimateDiff. As shown in the first row of Figure 6, the baseline method often suffers from structural and texture inconsistencies. For instance, the dog’s hindquarters exhibit an unnatural tail, and its facial features appear blurry. When the Structure Propagation Module (SPM) is introduced (second row of Figure 6), the structural coherence of the dog improves significantly, leading to an increase of 4.6 and 10.5 in CLIP-I and DINO scores, respectively. However, texture inconsistencies remain—for example, the dog’s face morphs into that of a

different breed. After incorporating the Texture Propagation Module (TPM), the dog’s facial texture becomes more consistent, further enhancing subject fidelity across frames.

Although the consistency of structure and texture has been significantly improved at this stage, fine-grained details, such as the dog’s color, still exhibit discrepancies compared to the reference subject. To address this issue, we further introduce the test-time reward optimization method. As shown in the fourth row of Figure 6, after optimizing the latent representation, the dog’s color distribution becomes more aligned with the reference subject, leading to further improvements in CLIP-I and DINO scores. The above analysis demonstrates that the proposed structure and texture propagation module, along with the test-time optimization method, effectively enhances the stability and consistency of customized video generation, advancing AI-driven storytelling video creation.

SPM	TPM	Reward	CLIP-T \uparrow	CLIP-I \uparrow	DINO \uparrow
			29.8	72.2	49.5
✓			31.1	76.8	61.0
	✓		31.0	77.1	59.1
✓	✓		31.4	78.9	61.1
✓	✓	✓	31.7	80.0	62.6

Table 2. The quantitative results of using different combinations of components.

6. Limitation and Conclusion

Limitation. Despite the improvement in maintaining subject consistency in videos, our approach still faces several limitations. First, the method struggles with personalized human subject generation. Since humans contain rich and intricate details, such as facial features and contours, the current approach finds it challenging to accurately capture and represent these fine-grained attributes. A potential solution is to incorporate prior knowledge of facial and body structures to enhance detail representation. Additionally, the length of generated videos remains relatively limited. To address this, integrating our approach with long-form video generation techniques could be a promising direction to improve the model’s capability in producing extended video sequences.

Conclusion. This paper primarily explores methods to enhance the consistency of customized video generation. While significant progress has been made in customized text-to-image (T2I) generation, directly integrating motion models for video generation often results in the loss of structural and texture information. To address this issue, we propose an autoregressive structure and texture propagation module. Experimental results demonstrate that our method effectively extracts the structural and texture information of the customized subject and propagates it across video frames, thereby

improving overall consistency. Furthermore, we introduce a reward optimization method to refine fine-grained details, validating the feasibility of test-time optimization.

References

- [1] Yogesh Balaji, Seungjun Nah, Xun Huang, Arash Vahdat, Jiaming Song, Qinsheng Zhang, Karsten Kreis, Miika Aittala, Timo Aila, Samuli Laine, et al. ediff-i: Text-to-image diffusion models with an ensemble of expert denoisers. *arXiv preprint arXiv:2211.01324*, 2022. 3, 5
- [2] Andreas Blattmann, Tim Dockhorn, Sumith Kulal, Daniel Mendelevitch, Maciej Kilian, Dominik Lorenz, Yam Levi, Zion English, Vikram Voleti, Adam Letts, et al. Stable video diffusion: Scaling latent video diffusion models to large datasets. *arXiv preprint arXiv:2311.15127*, 2023. 1, 2, 3
- [3] Andreas Blattmann, Robin Rombach, Huan Ling, Tim Dockhorn, Seung Wook Kim, Sanja Fidler, and Karsten Kreis. Align your latents: High-resolution video synthesis with latent diffusion models. In *Proceedings of the IEEE/CVF conference on computer vision and pattern recognition*, pages 22563–22575, 2023. 1
- [4] Hila Chefer, Shiran Zada, Roni Paiss, Ariel Ephrat, Omer Tov, Michael Rubinstein, Lior Wolf, Tali Dekel, Tomer Michaeli, and Inbar Mosseri. Still-moving: Customized video generation without customized video data. *ACM Transactions on Graphics (TOG)*, 43(6):1–11, 2024. 1, 2, 4
- [5] Hong Chen, Xin Wang, Guanning Zeng, Yipeng Zhang, Yuwei Zhou, Feilin Han, and Wenwu Zhu. Videodreamer: Customized multi-subject text-to-video generation with disen-mix finetuning. *arXiv preprint arXiv:2311.00990*, 2023. 2
- [6] Jianqi Chen, Panwen Hu, Xiaojun Chang, Zhenwei Shi, Michael Christian Kampffmeyer, and Xiaodan Liang. Sitcom-crafter: A plot-driven human motion generation system in 3d scenes. *arXiv preprint arXiv:2410.10790*, 2024. 1
- [7] Li Chen, Mengyi Zhao, Yiheng Liu, Mingxu Ding, Yangyang Song, Shizun Wang, Xu Wang, Hao Yang, Jing Liu, Kang Du, et al. Photoverse: Tuning-free image customization with text-to-image diffusion models. *arXiv preprint arXiv:2309.05793*, 2023. 2, 3
- [8] Seokju Cho, Sunghwan Hong, Sangryul Jeon, Yunsung Lee, Kwanghoon Sohn, and Seungryong Kim. Cats: Cost aggregation transformers for visual correspondence. *Advances in Neural Information Processing Systems*, 34:9011–9023, 2021. 4, 5
- [9] Rinon Gal, Yuval Alaluf, Yuval Atzmon, Or Patashnik, Amit H Bermano, Gal Chechik, and Daniel Cohen-Or. An image is worth one word: Personalizing text-to-image generation using textual inversion. *arXiv preprint arXiv:2208.01618*, 2022. 1, 2, 3, 4
- [10] Yuwei Guo, Ceyuan Yang, Anyi Rao, Zhengyang Liang, Yaohui Wang, Yu Qiao, Maneesh Agrawala, Dahua Lin, and Bo Dai. Animatediff: Animate your personalized text-to-image diffusion models without specific tuning. *arXiv preprint arXiv:2307.04725*, 2023. 3
- [11] Ligong Han, Yinxiao Li, Han Zhang, Peyman Milanfar, Dimitris Metaxas, and Feng Yang. Svdiff: Compact parameter space for diffusion fine-tuning. In *Proceedings of the IEEE/CVF International Conference on Computer Vision*, pages 7323–7334, 2023. 2
- [12] Shaozhe Hao, Kai Han, Shihao Zhao, and Kwan-Yee K Wong. Vico: Plug-and-play visual condition for personalized text-to-image generation. *arXiv preprint arXiv:2306.00971*, 2023. 2, 3, 6
- [13] Xuanhua He, Quande Liu, Shengju Qian, Xin Wang, Tao Hu, Ke Cao, Keyu Yan, and Jie Zhang. Id-animator: Zero-shot identity-preserving human video generation. *arXiv preprint arXiv:2404.15275*, 2024. 1, 2, 3
- [14] Yingqing He, Tianyu Yang, Yong Zhang, Ying Shan, and Qifeng Chen. Latent video diffusion models for high-fidelity long video generation. *arXiv preprint arXiv:2211.13221*, 2022. 1, 6
- [15] Amir Hertz, Ron Mokady, Jay Tenenbaum, Kfir Aberman, Yael Pritch, and Daniel Cohen-Or. Prompt-to-prompt image editing with cross attention control. *arXiv preprint arXiv:2208.01626*, 2022. 3
- [16] Sunghwan Hong, Jisu Nam, Seokju Cho, Susung Hong, Sangryul Jeon, Dongbo Min, and Seungryong Kim. Neural matching fields: Implicit representation of matching fields for visual correspondence. *Advances in Neural Information Processing Systems*, 35:13512–13526, 2022. 4, 5
- [17] Roger A Horn. The hadamard product. In *Proc. symp. appl. math*, pages 87–169, 1990. 6
- [18] Panwen Hu, Nan Xiao, Feifei Li, Yongquan Chen, and Rui Huang. A reinforcement learning-based automatic video editing method using pre-trained vision-language model. In *Proceedings of the 31st ACM International Conference on Multimedia*, pages 6441–6450, 2023. 1
- [19] Panwen Hu, Jin Jiang, Jianqi Chen, Mingfei Han, Shengcai Liao, Xiaojun Chang, and Xiaodan Liang. Storyagent: Customized storytelling video generation via multi-agent collaboration. *arXiv preprint arXiv:2411.04925*, 2024. 1, 2
- [20] Yuming Jiang, Tianxing Wu, Shuai Yang, Chenyang Si, Dahua Lin, Yu Qiao, Chen Change Loy, and Ziwei Liu. Videobooth: Diffusion-based video generation with image prompts. In *Proceedings of the IEEE/CVF Conference on Computer Vision and Pattern Recognition*, pages 6689–6700, 2024. 1, 2, 3, 6, 7
- [21] Hengjia Li, Haonan Qiu, Shiwei Zhang, Xiang Wang, Yujie Wei, Zekun Li, Yingya Zhang, Boxi Wu, and Deng Cai. Personalvideo: High id-fidelity video customization without dynamic and semantic degradation. *arXiv preprint arXiv:2411.17048*, 2024. 2
- [22] Zhiheng Liu, Ruili Feng, Kai Zhu, Yifei Zhang, Kecheng Zheng, Yu Liu, Deli Zhao, Jingren Zhou, and Yang Cao. Cones: Concept neurons in diffusion models for customized generation. *arXiv preprint arXiv:2303.05125*, 2023. 2
- [23] Fuchen Long, Zhaofan Qiu, Ting Yao, and Tao Mei. Videostudio: Generating consistent-content and multi-scene videos. In *European Conference on Computer Vision*, pages 468–485. Springer, 2024. 2, 6, 7

- [24] Ze Ma, Daquan Zhou, Chun-Hsiao Yeh, Xue-She Wang, Xiyu Li, Huanrui Yang, Zhen Dong, Kurt Keutzer, and Jiashi Feng. Magic-me: Identity-specific video customized diffusion. *arXiv preprint arXiv:2402.09368*, 2024. 2, 3, 6, 8
- [25] Jisu Nam, Heesu Kim, DongJae Lee, Siyoon Jin, Seungryong Kim, and Seunggyu Chang. Dreammatcher: appearance matching self-attention for semantically-consistent text-to-image personalization. In *Proceedings of the IEEE/CVF Conference on Computer Vision and Pattern Recognition*, pages 8100–8110, 2024. 2, 6
- [26] Lianyu Pang, Jian Yin, Baoquan Zhao, Feize Wu, Fu Lee Wang, Qing Li, and Xudong Mao. Attdreambooth: Towards text-aligned personalized text-to-image generation. *Advances in Neural Information Processing Systems*, 37:39869–39900, 2024. 2
- [27] Alec Radford, Jong Wook Kim, Chris Hallacy, Aditya Ramesh, Gabriel Goh, Sandhini Agarwal, Girish Sastry, Amanda Askell, Pamela Mishkin, Jack Clark, et al. Learning transferable visual models from natural language supervision. In *International conference on machine learning*, pages 8748–8763. PmLR, 2021. 6
- [28] Tianhe Ren, Shilong Liu, Ailing Zeng, Jing Lin, Kunchang Li, He Cao, Jiayu Chen, Xinyu Huang, Yukang Chen, Feng Yan, Zhaoyang Zeng, Hao Zhang, Feng Li, Jie Yang, Hongyang Li, Qing Jiang, and Lei Zhang. Grounded sam: Assembling open-world models for diverse visual tasks, 2024. 6
- [29] Weiming Ren, Huan Yang, Ge Zhang, Cong Wei, Xinrui Du, Wenhao Huang, and Wenhui Chen. Consistiv2: Enhancing visual consistency for image-to-video generation. *arXiv preprint arXiv:2402.04324*, 2024. 2
- [30] Robin Rombach, Andreas Blattmann, Dominik Lorenz, Patrick Esser, and Björn Ommer. High-resolution image synthesis with latent diffusion models, 2021. 3
- [31] Nataniel Ruiz, Yuanzhen Li, Varun Jampani, Yael Pritch, Michael Rubinstein, and Kfir Aberman. Dreambooth: Fine tuning text-to-image diffusion models for subject-driven generation. In *Proceedings of the IEEE/CVF conference on computer vision and pattern recognition*, pages 22500–22510, 2023. 1, 2, 3, 4, 7
- [32] D She, Mushui Liu, Jingxuan Pang, Jin Wang, Zhen Yang, Wanggui He, Guanghao Zhang, Yi Wang, Qihan Huang, Haobin Tang, et al. Customvideox: 3d reference attention driven dynamic adaptation for zero-shot customized video diffusion transformers. *arXiv preprint arXiv:2502.06527*, 2025. 1
- [33] Jiaming Song, Chenlin Meng, and Stefano Ermon. Denoising diffusion implicit models. *arXiv preprint arXiv:2010.02502*, 2020. 3, 6
- [34] Luming Tang, Menglin Jia, Qianqian Wang, Cheng Perng Phoo, and Bharath Hariharan. Emergent correspondence from image diffusion. *Advances in Neural Information Processing Systems*, 36:1363–1389, 2023. 5
- [35] Yoav Tewel, Rinon Gal, Gal Chechik, and Yuval Atzmon. Key-locked rank one editing for text-to-image personalization. In *ACM SIGGRAPH 2023 conference proceedings*, pages 1–11, 2023. 3
- [36] Prune Truong, Martin Danelljan, Radu Timofte, and Luc Van Gool. Pdc-net+: Enhanced probabilistic dense correspondence network. *IEEE Transactions on Pattern Analysis and Machine Intelligence*, 45(8):10247–10266, 2023. 4, 5
- [37] Narek Tumanyan, Michal Geyer, Shai Bagon, and Tali Dekel. Plug-and-play diffusion features for text-driven image-to-image translation. In *Proceedings of the IEEE/CVF Conference on Computer Vision and Pattern Recognition*, pages 1921–1930, 2023. 3
- [38] Cong Wang, Jiayi Gu, Panwen Hu, Songcen Xu, Hang Xu, and Xiaodan Liang. Dreamvideo: High-fidelity image-to-video generation with image retention and text guidance. *arXiv preprint arXiv:2312.03018*, 2023. 1
- [39] Cong Wang, Jiayi Gu, Panwen Hu, Haoyu Zhao, Yuanfan Guo, Jianhua Han, Hang Xu, and Xiaodan Liang. Easycontrol: Transfer controlnet to video diffusion for controllable generation and interpolation. *arXiv preprint arXiv:2408.13005*, 2024. 1
- [40] Cong Wang, Panwen Hu, Haoyu Zhao, Yuanfan Guo, Jiayi Gu, Xiao Dong, Jianhua Han, Hang Xu, and Xiaodan Liang. Uniadapter: All-in-one control for flexible video generation. *IEEE Transactions on Circuits and Systems for Video Technology*, 2025. 1
- [41] Xiaowei Wang, Siming Fu, Qihan Huang, Wanggui He, and Hao Jiang. Ms-diffusion: Multi-subject zero-shot image personalization with layout guidance. *arXiv preprint arXiv:2406.07209*, 2024. 6
- [42] Yaohui Wang, Xinyuan Chen, Xin Ma, Shangchen Zhou, Ziqi Huang, Yi Wang, Ceyuan Yang, Yanan He, Jiashuo Yu, Peiqing Yang, et al. Lavi: High-quality video generation with cascaded latent diffusion models. *International Journal of Computer Vision*, pages 1–20, 2024. 1
- [43] Zhao Wang, Aoxue Li, Lingting Zhu, Yong Guo, Qi Dou, and Zhenguang Li. Customvideo: Customizing text-to-video generation with multiple subjects. *arXiv preprint arXiv:2401.09962*, 2024. 2, 6
- [44] Zhenzhi Wang, Yixuan Li, Yanhong Zeng, Youqing Fang, Yuwei Guo, Wenran Liu, Jing Tan, Kai Chen, Tianfan Xue, Bo Dai, et al. Humanvid: Demystifying training data for camera-controllable human image animation. *Advances in Neural Information Processing Systems*, 37:20111–20131, 2025. 1
- [45] Yujie Wei, Shiwei Zhang, Zhiwu Qing, Hangjie Yuan, Zhiheng Liu, Yu Liu, Yingya Zhang, Jingren Zhou, and Hongming Shan. Dreamvideo: Composing your dream videos with customized subject and motion. In *Proceedings of the IEEE/CVF Conference on Computer Vision and Pattern Recognition*, pages 6537–6549, 2024. 1, 2, 3, 6, 7, 8
- [46] Tao Wu, Yong Zhang, Xintao Wang, Xianpan Zhou, Guangcong Zheng, Zhongang Qi, Ying Shan, and Xi Li. Customcrafter: Customized video generation with preserving motion and concept composition abilities. *arXiv preprint arXiv:2408.13239*, 2024. 2
- [47] Guangxuan Xiao, Tianwei Yin, William T Freeman, Frédo Durand, and Song Han. Fastcomposer: Tuning-free multi-subject image generation with localized attention. *International Journal of Computer Vision*, pages 1–20, 2024. 1

- [48] Jinbo Xing, Menghan Xia, Yong Zhang, Haoxin Chen, Wangbo Yu, Hanyuan Liu, Gongye Liu, Xintao Wang, Ying Shan, and Tien-Tsin Wong. Dynamicrafter: Animating open-domain images with video diffusion priors. In *European Conference on Computer Vision*, pages 399–417. Springer, 2024. [1](#), [2](#), [3](#)
- [49] Zhuoyi Yang, Jiayan Teng, Wendi Zheng, Ming Ding, Shiyu Huang, Jiazheng Xu, Yuanming Yang, Wenyi Hong, Xiaohan Zhang, Guanyu Feng, et al. Cogvideox: Text-to-video diffusion models with an expert transformer. *arXiv preprint arXiv:2408.06072*, 2024. [1](#)
- [50] Hao Zhang, Feng Li, Shilong Liu, Lei Zhang, Hang Su, Jun Zhu, Lionel M Ni, and Heung-Yeung Shum. Dino: Detr with improved denoising anchor boxes for end-to-end object detection. *arXiv preprint arXiv:2203.03605*, 2022. [7](#)
- [51] Junyi Zhang, Charles Herrmann, Junhwa Hur, Luisa Polania Cabrera, Varun Jampani, Deqing Sun, and Ming-Hsuan Yang. A tale of two features: Stable diffusion complements dino for zero-shot semantic correspondence. *Advances in Neural Information Processing Systems*, 36:45533–45547, 2023. [5](#)
- [52] Yuxuan Zhang, Yiren Song, Jiaming Liu, Rui Wang, Jinpeng Yu, Hao Tang, Huaxia Li, Xu Tang, Yao Hu, Han Pan, et al. Ssr-encoder: Encoding selective subject representation for subject-driven generation. In *Proceedings of the IEEE/CVF Conference on Computer Vision and Pattern Recognition*, pages 8069–8078, 2024. [6](#)
- [53] Zhenghao Zhang, Junchao Liao, Menghao Li, Zuozhuo Dai, Bingxue Qiu, Siyu Zhu, Long Qin, and Weizhi Wang. Tora: Trajectory-oriented diffusion transformer for video generation. *arXiv preprint arXiv:2407.21705*, 2024. [1](#)
- [54] Guangcong Zheng, Teng Li, Rui Jiang, Yehao Lu, Tao Wu, and Xi Li. Cami2v: Camera-controlled image-to-video diffusion model. *arXiv preprint arXiv:2410.15957*, 2024. [1](#)
- [55] Shaobin Zhuang, Kunchang Li, Xinyuan Chen, Yaohui Wang, Ziwei Liu, Yu Qiao, and Yali Wang. Vlogger: Make your dream a vlog. In *Proceedings of the IEEE/CVF Conference on Computer Vision and Pattern Recognition*, pages 8806–8817, 2024. [2](#)